Observation of the decay B- D(s)((*)+) K- - nu()

del Amo Sanchez, P.; Raven, H.G.; Snoek, H.; BaBar, Collaboration

published in
Physical Review Letters
2011

DOI (link to publisher)
10.1103/PhysRevLett.107.041804

document version
Publisher's PDF, also known as Version of record

citation for published version (APA)
del Amo Sanchez, P., Raven, H. G., Snoek, H., & BaBar, C. (2011). Observation of the decay B- D(s)((*)+) K- - nu(). *Physical Review Letters*, *107*(4), 041804. [041804]. https://doi.org/10.1103/PhysRevLett.107.041804

Observation of the Decay $B^- \to D_s^{(*)+} K^- \ell^- \bar{\nu}_\ell$

P. del Amo Sanchez,[1] J. P. Lees,[1] V. Poireau,[1] E. Prencipe,[1] V. Tisserand,[1] J. Garra Tico,[2] E. Grauges,[2] M. Martinelli,[3a,3b]
A. Palano,[3a,3b] M. Pappagallo,[3a,3b] G. Eigen,[4] B. Stugu,[4] L. Sun,[4] M. Battaglia,[5] D. N. Brown,[5] B. Hooberman,[5]
L. T. Kerth,[5] Yu. G. Kolomensky,[5] G. Lynch,[5] I. L. Osipenkov,[5] T. Tanabe,[5] C. M. Hawkes,[6] A. T. Watson,[6] H. Koch,[7]
T. Schroeder,[7] D. J. Asgeirsson,[8] C. Hearty,[8] T. S. Mattison,[8] J. A. McKenna,[8] A. Khan,[9] A. Randle-Conde,[9] V. E. Blinov,[10]
A. R. Buzykaev,[10] V. P. Druzhinin,[10] V. B. Golubev,[10] A. P. Onuchin,[10] S. I. Serednyakov,[10] Yu. I. Skovpen,[10]
E. P. Solodov,[10] K. Yu. Todyshev,[10] A. N. Yushkov,[10] M. Bondioli,[11] S. Curry,[11] D. Kirkby,[11] A. J. Lankford,[11]
M. Mandelkern,[11] E. C. Martin,[11] D. P. Stoker,[11] H. Atmacan,[12] J. W. Gary,[12] F. Liu,[12] O. Long,[12] G. M. Vitug,[12]
C. Campagnari,[13] T. M. Hong,[13] D. Kovalskyi,[13] J. D. Richman,[13] A. M. Eisner,[14] C. A. Heusch,[14] J. Kroseberg,[14]
W. S. Lockman,[14] A. J. Martinez,[14] T. Schalk,[14] B. A. Schumm,[14] A. Seiden,[14] L. O. Winstrom,[14] C. H. Cheng,[1]
D. A. Doll,[1] B. Echenard,[1] D. G. Hitlin,[1] P. Ongmongkolkul,[1] F. C. Porter,[1] A. Y. Rakitin,[1] R. Andreassen,[16]
M. S. Dubrovin,[16] G. Mancinelli,[16] B. T. Meadows,[16] M. D. Sokoloff,[16] P. C. Bloom,[2] W. T. Ford,[2] A. Gaz,[2] M. Nagel,[2]
U. Nauenberg,[2] J. G. Smith,[2] S. R. Wagner,[2] R. Ayad,[18,*] W. H. Toki,[18] H. Jasper,[19] T. M. Karbach,[19] J. Merkel,[19]
A. Petzold,[19] B. Spaan,[19] K. Wacker,[19] M. J. Kobel,[20] K. R. Schubert,[20] R. Schwierz,[20] D. Bernard,[21] M. Verderi,[21]
P. J. Clark,[22] S. Playfer,[22] J. E. Watson,[22] M. Andreotti,[23a,23b] D. Bettoni,[23a] C. Bozzi,[23a] R. Calabrese,[23a,23b]
A. Cecchi,[23a,23b] G. Cibinetto,[23a,23b] E. Fioravanti,[23a,23b] P. Franchini,[23a,23b] E. Luppi,[23a,23b] M. Munerato,[23a,23b]
M. Negrini,[23a,23b] A. Petrella,[23a,23b] L. Piemontese,[23a] R. Baldini-Ferroli,[24] A. Calcaterra,[24] R. de Sangro,[24]
G. Finocchiaro,[24] M. Nicolaci,[24] S. Pacetti,[24] P. Patteri,[24] I. M. Peruzzi,[24,†] M. Piccolo,[24] M. Rama,[24] A. Zallo,[24]
R. Contri,[25a,25b] E. Guido,[25a,25b] M. Lo Vetere,[25a,25b] M. R. Monge,[25a,25b] S. Passaggio,[25a] C. Patrignani,[25a,25b]
E. Robutti,[25a] S. Tosi,[25a,25b] B. Bhuyan,[26] V. Prasad,[26] C. L. Lee,[27] M. Morii,[27] A. Adametz,[28] J. Marks,[28] S. Schenk,[28]
U. Uwer,[28] F. U. Bernlochner,[29] M. Ebert,[29] H. M. Lacker,[29] T. Lueck,[29] A. Volk,[29] P. D. Dauncey,[30] M. Tibbetts,[30]
P. K. Behera,[31] U. Mallik,[31] C. Chen,[32] J. Cochran,[32] H. B. Crawley,[32] L. Dong,[32] W. T. Meyer,[32] S. Prell,[32]
E. I. Rosenberg,[32] A. E. Rubin,[32] Y. Y. Gao,[33] A. V. Gritsan,[33] Z. J. Guo,[33] N. Arnaud,[34] M. Davier,[34] D. Derkach,[34]
J. Firmino da Costa,[34] G. Grosdidier,[34] F. Le Diberder,[34] A. M. Lutz,[34] B. Malaescu,[34] A. Perez,[34] P. Roudeau,[34]
M. H. Schune,[34] J. Serrano,[34] V. Sordini,[34,‡] A. Stocchi,[34] L. Wang,[34] G. Wormser,[34] D. J. Lange,[35] D. M. Wright,[35]
I. Bingham,[36] C. A. Chavez,[36] J. P. Coleman,[36] J. R. Fry,[36] E. Gabathuler,[36] R. Gamet,[36] D. E. Hutchcroft,[36] D. J. Payne,[36]
C. Touramanis,[36] A. J. Bevan,[37] F. Di Lodovico,[37] R. Sacco,[37] M. Sigamani,[38] G. Cowan,[38] S. Paramesvaran,[38]
A. C. Wren,[38] D. N. Brown,[39] C. L. Davis,[39] A. G. Denig,[40] M. Fritsch,[40] W. Gradl,[40] A. Hafner,[40] K. E. Alwyn,[41]
D. Bailey,[41] R. J. Barlow,[41] G. Jackson,[41] G. D. Lafferty,[41] T. J. West,[41] J. Anderson,[42] R. Cenci,[42] A. Jawahery,[42]
D. A. Roberts,[42] G. Simi,[42] J. M. Tuggle,[42] C. Dallapiccola,[43] E. Salvati,[43] R. Cowan,[44] D. Dujmic,[44] P. H. Fisher,[44]
G. Sciolla,[44] M. Zhao,[44] D. Lindemann,[45] P. M. Patel,[45] S. H. Robertson,[45] M. Schram,[45] P. Biassoni,[46a,46a]
A. Lazzaro,[46a,46a] V. Lombardo,[46a] F. Palombo,[46a,46a] S. Stracka,[46a,46a] L. Cremaldi,[47] R. Godang,[47,§] R. Kroeger,[47]
P. Sonnek,[47] D. J. Summers,[47] X. Nguyen,[48] M. Simard,[48] P. Taras,[48] G. De Nardo,[49a,49b] D. Monorchio,[49a,49b]
G. Onorato,[49a,49b] C. Sciacca,[49a] G. Raven,[50] H. L. Snoek,[50] C. P. Jessop,[51] K. J. Knoepfel,[51] J. M. LoSecco,[51]
W. F. Wang,[51] L. A. Corwin,[52] K. Honscheid,[52] R. Kass,[52] J. P. Morris,[52] A. M. Rahimi,[52] N. L. Blount,[53] J. Brau,[53]
R. Frey,[53] O. Igonkina,[53] J. A. Kolb,[53] R. Rahmat,[53] N. B. Sinev,[53] D. Strom,[53] J. Strube,[53] E. Torrence,[53] G. Castelli,[54a,54b]
E. Feltresi,[54a,54b] N. Gagliardi,[54a,54b] M. Margoni,[54a,54b] M. Morandin,[54a] M. Posocco,[54a] M. Rotondo,[54a]
F. Simonetto,[54a,54b] R. Stroili,[54a,54b] E. Ben-Haim,[55] G. R. Bonneaud,[55] H. Briand,[55] G. Calderini,[55] J. Chauveau,[55]
O. Hamon,[55] Ph. Leruste,[55] G. Marchiori,[55] J. Ocariz,[55] J. Prendki,[55] S. Sitt,[55] M. Biasini,[56a,56b] E. Manoni,[56a,56b]
A. Rossi,[56a,56b] C. Angelini,[57a,57b] G. Batignani,[57a,57b] S. Bettarini,[57a,57b] M. Carpinelli,[57a,57b,||] G. Casarosa,[57a,57b]
A. Cervelli,[57a,57b] F. Forti,[57a,57b] M. A. Giorgi,[57a,57b] A. Lusiani,[57a] N. Neri,[57a] E. Paoloni,[57a,57b] G. Rizzo,[57a,57b]
J. J. Walsh,[57a] D. Lopes Pegna,[58] C. Lu,[58] J. Olsen,[58] A. J. S. Smith,[58] A. V. Telnov,[58] F. Anulli,[59a] E. Baracchini,[59a,59b]
G. Cavoto,[59a] R. Faccini,[59a,59b] F. Ferrarotto,[59a,59b] F. Ferroni,[59a,59b] M. Gaspero,[59a,59b] L. Li Gioi,[59a] M. A. Mazzoni,[59a]
G. Piredda,[59a] F. Renga,[59a,59b] T. Hartmann,[60] T. Leddig,[60] H. Schröder,[60] R. Waldi,[60] T. Adye,[61] B. Franek,[61]
E. O. Olaiya,[61] F. F. Wilson,[61] S. Emery,[62] G. Hamel de Monchenault,[62] G. Vasseur,[62] Ch. Yèche,[62] M. Zito,[62]
M. T. Allen,[63] D. Aston,[63] D. J. Bard,[63] R. Bartoldus,[63] J. F. Benitez,[63] C. Cartaro,[63] M. R. Convery,[63] J. Dorfan,[63]
G. P. Dubois-Felsmann,[63] W. Dunwoodie,[63] R. C. Field,[63] M. Franco Sevilla,[63] B. G. Fulsom,[63] A. M. Gabareen,[63]
M. T. Graham,[63] P. Grenier,[63] C. Hast,[63] W. R. Innes,[63] M. H. Kelsey,[63] H. Kim,[63] P. Kim,[63] M. L. Kocian,[63]
D. W. G. S. Leith,[63] S. Li,[63] B. Lindquist,[63] S. Luitz,[63] V. Luth,[63] H. L. Lynch,[63] D. B. MacFarlane,[63] H. Marsiske,[63]

0031-9007/11/107(4)/041804(8)

D. R. Muller,[63] H. Neal,[63] S. Nelson,[63] C. P. O'Grady,[63] I. Ofte,[63] M. Perl,[63] T. Pulliam,[63] B. N. Ratcliff,[63] A. Roodman,[63] A. A. Salnikov,[63] V. Santoro,[63] R. H. Schindler,[63] J. Schwiening,[63] A. Snyder,[63] D. Su,[63] M. K. Sullivan,[63] S. Sun,[63] K. Suzuki,[63] J. M. Thompson,[63] J. Va'vra,[63] A. P. Wagner,[63] M. Weaver,[63] C. A. West,[63] W. J. Wisniewski,[63] M. Wittgen,[63] D. H. Wright,[63] H. W. Wulsin,[63] A. K. Yarritu,[63] C. C. Young,[63] V. Ziegler,[63] X. R. Chen,[64] W. Park,[64] M. V. Purohit,[64] R. M. White,[64] J. R. Wilson,[64] S. J. Sekula,[65] M. Bellis,[66] P. R. Burchat,[66] A. J. Edwards,[66] T. S. Miyashita,[66] S. Ahmed,[67] M. S. Alam,[67] J. A. Ernst,[67] B. Pan,[67] M. A. Saeed,[67] S. B. Zain,[67] N. Guttman,[68] A. Soffer,[68] P. Lund,[69] S. M. Spanier,[69] R. Eckmann,[70] J. L. Ritchie,[70] A. M. Ruland,[70] C. J. Schilling,[70] R. F. Schwitters,[70] B. C. Wray,[70] J. M. Izen,[71] X. C. Lou,[71] F. Bianchi,[72a,72b] D. Gamba,[72a,72b] M. Pelliccioni,[72a,72b] M. Bomben,[73a,73b] L. Lanceri,[73a,73b] L. Vitale,[73a,73b] N. Lopez-March,[74] F. Martinez-Vidal,[74] D. A. Milanes,[74] A. Oyanguren,[74] J. Albert,[75] Sw. Banerjee,[75] H. H. F. Choi,[75] K. Hamano,[75] G. J. King,[75] R. Kowalewski,[75] M. J. Lewczuk,[75] I. M. Nugent,[75] J. M. Roney,[75] R. J. Sobie,[75] T. J. Gershon,[76] P. F. Harrison,[76] T. E. Latham,[76] E. M. T. Puccio,[76] H. R. Band,[77] S. Dasu,[77] K. T. Flood,[77] Y. Pan,[77] R. Prepost,[77] C. O. Vuosalo,[77] and S. L. Wu[77]

(*BaBar* Collaboration)

[1]Laboratoire d'Annecy-le-Vieux de Physique des Particules (LAPP), Université de Savoie,
CNRS/IN2P3, F-74941 Annecy-Le-Vieux, France
[2]Universitat de Barcelona, Facultat de Fisica, Departament ECM, E-08028 Barcelona, Spain
[3a]INFN Sezione di Bari, I-70126 Bari, Italy
[3b]Dipartimento di Fisica, Università di Bari, I-70126 Bari, Italy
[4]University of Bergen, Institute of Physics, N-5007 Bergen, Norway
[5]Lawrence Berkeley National Laboratory and University of California, Berkeley, California 94720, USA
[6]University of Birmingham, Birmingham, B15 2TT, United Kingdom
[7]Ruhr Universität Bochum, Institut für Experimentalphysik 1, D-44780 Bochum, Germany
[8]University of British Columbia, Vancouver, British Columbia, Canada V6T 1Z1
[9]Brunel University, Uxbridge, Middlesex UB8 3PH, United Kingdom
[10]Budker Institute of Nuclear Physics, Novosibirsk 630090, Russia
[11]University of California at Irvine, Irvine, California 92697, USA
[12]University of California at Riverside, Riverside, California 92521, USA
[13]University of California at Santa Barbara, Santa Barbara, California 93106, USA
[14]University of California at Santa Cruz, Institute for Particle Physics, Santa Cruz, California 95064, USA
[1]California Institute of Technology, Pasadena, California 91125, USA
[16]University of Cincinnati, Cincinnati, Ohio 45221, USA
[2]University of Colorado, Boulder, Colorado 80309, USA
[18]Colorado State University, Fort Collins, Colorado 80523, USA
[19]Technische Universität Dortmund, Fakultät Physik, D-44221 Dortmund, Germany
[20]Technische Universität Dresden, Institut für Kern- und Teilchenphysik, D-01062 Dresden, Germany
[21]Laboratoire Leprince-Ringuet, CNRS/IN2P3, Ecole Polytechnique, F-91128 Palaiseau, France
[22]University of Edinburgh, Edinburgh EH9 3JZ, United Kingdom
[23a]INFN Sezione di Ferrara, I-44100 Ferrara, Italy
[23b]Dipartimento di Fisica, Università di Ferrara, I-44100 Ferrara, Italy
[24]INFN Laboratori Nazionali di Frascati, I-00044 Frascati, Italy
[25a]INFN Sezione di Genova, I-16146 Genova, Italy
[25b]Dipartimento di Fisica, Università di Genova, I-16146 Genova, Italy
[26]Indian Institute of Technology Guwahati, Guwahati, Assam, 781 039, India
[27]Harvard University, Cambridge, Massachusetts 02138, USA
[28]Universität Heidelberg, Physikalisches Institut, Philosophenweg 12, D-69120 Heidelberg, Germany
[29]Humboldt-Universität zu Berlin, Institut für Physik, Newtonstrasse 15, D-12489 Berlin, Germany
[30]Imperial College London, London, SW7 2AZ, United Kingdom
[31]University of Iowa, Iowa City, Iowa 52242, USA
[32]Iowa State University, Ames, Iowa 50011-3160, USA
[33]Johns Hopkins University, Baltimore, Maryland 21218, USA
[34]Laboratoire de l'Accélérateur Linéaire, IN2P3/CNRS et Université Paris-Sud 11,
Centre Scientifique d'Orsay, B.P. 34, F-91898 Orsay Cedex, France
[35]Lawrence Livermore National Laboratory, Livermore, California 94550, USA
[36]University of Liverpool, Liverpool L69 7ZE, United Kingdom
[37]Queen Mary, University of London, London, E1 4NS, United Kingdom
[38]University of London, Royal Holloway and Bedford New College, Egham, Surrey TW20 0EX, United Kingdom

[39]*University of Louisville, Louisville, Kentucky 40292, USA*
[40]*Johannes Gutenberg-Universität Mainz, Institut für Kernphysik, D-55099 Mainz, Germany*
[41]*University of Manchester, Manchester M13 9PL, United Kingdom*
[42]*University of Maryland, College Park, Maryland 20742, USA*
[43]*University of Massachusetts, Amherst, Massachusetts 01003, USA*
[44]*Massachusetts Institute of Technology, Laboratory for Nuclear Science, Cambridge, Massachusetts 02139, USA*
[45]*McGill University, Montréal, Québec, Canada H3A 2T8*
[46a]*INFN Sezione di Milano, I-20133 Milano, Italy*
[46a]*Dipartimento di Fisica, Università di Milano, I-20133 Milano, Italy*
[47]*University of Mississippi, University, Mississippi 38677, USA*
[48]*Université de Montréal, Physique des Particules, Montréal, Québec, Canada H3C 3J7*
[49a]*INFN Sezione di Napol, I-80126 Napoli, Italy*
[49b]*Dipartimento di Scienze Fisiche, Università di Napoli Federico II, I-80126 Napoli, Italy*
[50]*NIKHEF, National Institute for Nuclear Physics and High Energy Physics, NL-1009 DB Amsterdam, The Netherlands*
[51]*University of Notre Dame, Notre Dame, Indiana 46556, USA*
[52]*Ohio State University, Columbus, Ohio 43210, USA*
[53]*University of Oregon, Eugene, Oregon 97403, USA*
[54a]*INFN Sezione di Padova, I-35131 Padova, Italy*
[54b]*Dipartimento di Fisica, Università di Padova, I-35131 Padova, Italy*
[55]*Laboratoire de Physique Nucléaire et de Hautes Energies, IN2P3/CNRS, Université Pierre et Marie Curie-Paris6,*
Université Denis Diderot-Paris7, F-75252 Paris, France
[56a]*INFN Sezione di Perugia, I-06100 Perugia, Italy*
[56b]*Dipartimento di Fisica, Università di Perugia, I-06100 Perugia, Italy*
[57a]*INFN Sezione di Pisa, I-56127 Pisa, Italy*
[57b]*Dipartimento di Fisica, Università di Pisa, I-56127 Pisa, Italy*
[57c]*Scuola Normale Superiore di Pisa, I-56127 Pisa, Italy*
[58]*Princeton University, Princeton, New Jersey 08544, USA*
[59a]*INFN Sezione di Roma, I-00185 Roma, Italy*
[59b]*Dipartimento di Fisica, Università di Roma La Sapienza, I-00185 Roma, Italy*
[60]*Universität Rostock, D-18051 Rostock, Germany*
[61]*Rutherford Appleton Laboratory, Chilton, Didcot, Oxon, OX11 0QX, United Kingdom*
[62]*CEA, Irfu, SPP, Centre de Saclay, F-91191 Gif-sur-Yvette, France*
[63]*SLAC National Accelerator Laboratory, Stanford, California 94309 USA*
[64]*University of South Carolina, Columbia, South Carolina 29208, USA*
[65]*Southern Methodist University, Dallas, Texas 75275, USA*
[66]*Stanford University, Stanford, California 94305-4060, USA*
[67]*State University of New York, Albany, New York 12222, USA*
[68]*Tel Aviv University, School of Physics and Astronomy, Tel Aviv, 69978, Israel*
[69]*University of Tennessee, Knoxville, Tennessee 37996, USA*
[70]*University of Texas at Austin, Austin, Texas 78712, USA*
[71]*University of Texas at Dallas, Richardson, Texas 75083, USA*
[72a]*INFN Sezione di Torino, I-10125 Torino, Italy*
[72b]*Dipartimento di Fisica Sperimentale, Università di Torino, I-10125 Torino, Italy*
[73a]*INFN Sezione di Trieste, I-34127 Trieste, Italy*
[73b]*Dipartimento di Fisica, Università di Trieste, I-34127 Trieste, Italy*
[74]*IFIC, Universitat de Valencia-CSIC, E-46071 Valencia, Spain*
[75]*University of Victoria, Victoria, British Columbia, Canada V8W 3P6*
[76]*Department of Physics, University of Warwick, Coventry CV4 7AL, United Kingdom*
[77]*University of Wisconsin, Madison, Wisconsin 53706, USA*

(Received 22 December 2010; published 22 July 2011)

We report the observation of the decay $B^- \to D_s^{(*)+} K^- \ell^- \bar{\nu}_\ell$ based on 342 fb^{-1} of data collected at the $\Upsilon(4S)$ resonance with the *BABAR* detector at the PEP-II e^+e^- storage rings at SLAC. A simultaneous fit to three D_s^+ decay chains is performed to extract the signal yield from measurements of the squared missing mass in the B meson decay. We observe the decay $B^- \to D_s^{(*)+} K^- \ell^- \bar{\nu}_\ell$ with a significance greater than 5 standard deviations (including systematic uncertainties) and measure its branching fraction to be $\mathcal{B}(B^- \to D_s^{(*)+} K^- \ell^- \bar{\nu}_\ell) = [6.13^{+1.04}_{-1.03}(\text{stat}) \pm 0.43(\text{syst}) \pm 0.51(\mathcal{B}(D_s))] \times 10^{-4}$, where the last error reflects the limited knowledge of the D_s branching fractions.

DOI: 10.1103/PhysRevLett.107.041804 PACS numbers: 13.20.He, 12.15.Ji, 12.38.Qk

The study of charmed inclusive semileptonic B meson decays enables the measurement of the Cabibbo-Kobayashi-Maskawa matrix element $|V_{cb}|$. This measurement relies on a precise knowledge of all semileptonic B meson decays. Decays of orbitally excited D mesons, from the process $B \to D^{**}\ell\nu$, constitute a significant fraction of these decays [1] and may help explain the discrepancy between the inclusive $B \to X_c \ell\nu$ rate, where X_c is a charmed hadronic final state, and the sum of the measured exclusive decay rates [1,2]. So far, analyses of these decays have focused on the reconstruction of $B \to D^{(*)}\pi\ell\nu$ states [3–5]. In such analyses, experimental data are interpreted as a sum of the four D^{**} resonances. The results show the dominance of B decays to broad resonances, while QCD sum rules imply the opposite [6]. Conversely, a small contribution from broad D^{**} states implies the presence of a nonresonant $B \to D^{(*)}\pi\ell\nu$ component, which has not yet been observed. Measurement of the branching fraction for the as-yet-unobserved $B^- \to D_s^{(*)+}K^-\ell^-\bar{\nu}_\ell$ decay [7] would provide additional information relevant to this issue, by exploring the hadronic mass distribution above 2.46 GeV/c^2 where resonant and nonresonant components are present. In addition, the measurement of $B^- \to D_s^{(*)+}K^-\ell^-\bar{\nu}_\ell$ will provide a better estimate of background in future studies of semileptonic $\bar{B}_s \to D_s^+ X\ell^-\bar{\nu}_\ell$ decays.

By using the shape of the hadronic mass spectrum in B semileptonic decays, a rough estimate on the branching fraction $\mathcal{B}(B^- \to D_s^{(*)+}K^-\ell^-\bar{\nu}_\ell)$ is of the order of 10^{-3} [8,9], which is consistent with the limit set by the ARGUS Collaboration, $\mathcal{B}(B^- \to D_s^{(*)+}K^-\ell^-\bar{\nu}_\ell) < 5 \times 10^{-3}$ at 90% confidence level [10]. A comparison between this expectation and the actual measurement can confirm or refute the expected rapid decrease of the hadronic mass distribution at high values.

In this Letter, we present the observation of $B^- \to D_s^{(*)+}K^-\ell^-\bar{\nu}_\ell$ decays, where $\ell = e, \mu$. This analysis does not differentiate between final states with D_s^+ and D_s^{*+}, where D_s^{*+} decays via emission of neutral decay products that are not reconstructed. The results are based on a data sample of $N_{B\bar{B}} = (376.9 \pm 4.1) \times 10^6$ $B\bar{B}$ pairs recorded at the $\Upsilon(4S)$ resonance with the *BABAR* detector [11] at the PEP-II asymmetric energy e^+e^- storage rings at the SLAC National Accelerator Laboratory. This corresponds to an integrated luminosity of 342 fb^{-1}. In addition, 37 fb^{-1} of data collected about 40 MeV below the resonance are used for background studies. A GEANT-based Monte Carlo (MC) simulation [12] of $B\bar{B}$ and continuum events ($e^+e^- \to q\bar{q}$ with $q = u, d, s, c$) is used to study the detector response and acceptance, validate the analysis technique, and evaluate signal efficiencies. The sample of simulated $B\bar{B}$ events is equivalent to approximately 3 times the data sample. The signal MC events are generated by adapting the decay model of Goity and Roberts [13] to describe $D_s^+K^-$ final states. Two alternative signal MC samples are used to estimate systematic uncertainties: a sample based on the ISGW2 model [14], in which B^- mesons decay to $D_0^{*0}\ell^-\bar{\nu}$ with $D_0^{*0} \to D_s^+K^-$, and a sample based on a simple phase space model. The signal MC samples are equivalent to approximately 10 times the expected signal yield.

We reconstruct D_s^+ candidates in three decay chains: $D_s^+ \to \phi\pi^+$ with $\phi \to K^+K^-$, $D_s^+ \to \bar{K}^{*0}K^+$ with $\bar{K}^{*0} \to K^-\pi^+$, and $D_s^+ \to K_S^0K^+$ with $K_S^0 \to \pi^+\pi^-$. The ϕ, $\bar{K}^{*0}$, and K_S^0 candidates are formed by combining oppositely charged tracks. To suppress combinatorial background from the D_s^+ reconstruction in the first two decay chains, we employ a feed-forward neural network (multilayer perceptron [15]) with three input variables and four hidden layers. The input variables are the absolute value of the difference between the reconstructed and the nominal mass values of the $\phi/\bar{K}^{*0}$ candidate [1], the absolute value of the cosine of the helicity angle of the $\phi/\bar{K}^{*0}$, and the χ^2 probability of the fit to the D_s^+ candidate. The helicity angle is defined as the angle between the D_s^+ candidate and one kaon originating from the $\phi/\bar{K}^{*0}$ in the $\phi/\bar{K}^{*0}$ rest frame. To suppress combinatorial background in the $D_s^+ \to K_S^0K^+$ decay chain, we require the invariant mass of the charged pions forming the K_S^0 candidate to satisfy $0.490\ \mathrm{GeV}/c^2 < m(\pi\pi) < 0.506\ \mathrm{GeV}/c^2$, the flight length of the K_S^0 to be larger than 1 mm, the cosine of the laboratory angle between the K_S^0 momentum and the line connecting the K_S^0 decay vertex and the primary vertex of the event to be positive, and the probability of the D_s^+ candidate's vertex fit to be larger than 0.001. The selection criteria are optimized to maximize the statistical significance of the signal. No requirement on the mass of the D_s^+ candidates is applied, since this distribution is used to extract the signal yield.

A lepton and a kaon, both with negative charge, are combined with the D_s^+ candidate to form a B^- candidate. Leptons are required to have momentum $|\vec{p}_\ell|$ larger than 0.8 GeV/c [16] to reject those not directly originating from B mesons. The probability of the vertex fit of the B candidate is required to be larger than 0.01.

Three event-shape variables that are sensitive to the topological differences between jetlike continuum events and more spherical $B\bar{B}$ events are used as input to a neural network to suppress background from continuum events. These variables are the normalized second Fox-Wolfram moment R_2 [17], the monomial L_2 [18], and the cosine of the angle between the flight direction of the reconstructed B candidate and the rest of the event. A neural network whose input variables are the B candidate mass, the B candidate sphericity, and the thrust value of the rest of the event is used to reduce the background from other B decays, providing a slight, but not negligible, improvement in the sensitivity of the measurement.

After applying these selection criteria, the remaining background events are divided into two classes, depending on whether or not they contain a correctly reconstructed D_s^+ meson. The first class is the more important of the two. We refer to it as D_s^+ background events in the following. Most of these events contain a D_s originating from decays such as $B \to D_s D$, where the kaon and lepton tracks used to form a B candidate are taken from the other B meson in the event. The angular correlation between the flight directions of the D_s and the D is used to suppress the D_s background candidates. The direction of the D meson is estimated from the direction of a previously unused charged or neutral kaon candidate that is assumed to be from $D \to K^{\pm,0}X$ decays. By requiring the cosine of the angle between the flight direction of the D_s candidate and the additional kaon to be larger than -0.5, about 30% of the D_s-background events are rejected, as shown in Fig. 1. About 8% of the remaining events have multiple candidates, predominantly two. In such cases, we choose the candidate with the largest B vertex fit probability.

The remaining events are divided into signal regions and sidebands based on the mass of the D_s^+ candidate. The sidebands are defined by $1.9\ \mathrm{GeV}/c^2 < m(D_s^+) < 1.94\ \mathrm{GeV}/c^2$ and $2.0\ \mathrm{GeV}/c^2 < m(D_s^+) < 2.04\ \mathrm{GeV}/c^2$. Fits to the D_s^+ mass distributions are performed separately for each decay channel to define the signal regions and to measure the number of reconstructed D_s^+ mesons, which are used later for extracting the signal yield. The signal regions are defined as $\pm 2.5\sigma$ wide bands, centered on the "fitted means" for each decay channel. Signal events are identified by the missing mass of the visible decay products $Y = D_s^+ K^- \ell^-$ with respect to the nominal B meson mass:

$$M_m^2 = (E_B - E_Y)^2 - |\vec{p}_Y|^2 = m_\nu^2, \tag{1}$$

where E_B is the beam energy, corresponding to the energy of the B meson, while E_Y and $\vec{p}_Y$ represent the energy and momentum of the Y composite, respectively. Because of its smallness and unknown direction, the momentum of the B meson is neglected. This leads to a distribution for M_m^2 with a Gaussian shape for correctly reconstructed signal events. Other B semileptonic decays, where one particle is not reconstructed or is erroneously included, lead to higher or lower values of M_m^2.

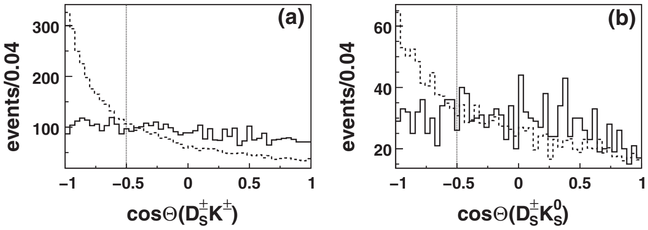

FIG. 1. Angular distribution of the cosine of the angle between the flight direction of the $D_s^\pm$ meson and additional charged and neutral kaons: (a) $\cos\Theta(D_s^\pm K^\pm)$ and (b) $\cos\Theta(D_s^\pm K_S^0)$. Solid lines represent signal MC events; dashed lines are D_s^+ background. The vertical lines indicate the selection applied.

To extract the signal yield, we perform an unbinned extended maximum-likelihood fit, applied simultaneously to the M_m^2 distributions of the signal region and the sidebands of the three D_s^+ decay chains. While the sidebands are populated only by combinatorial background events, the signal region also contains D_s^+ background and signal events. Because their lepton acceptances differ, the electron and muon channels are fitted separately. The combinatorial background is modeled by using a sum of two Gaussian distributions whose parameters are the same for the three D_s^+ decay chains. This parameterization is favored by MC simulation. This fit technique is equivalent to a sideband subtraction. The contributions of D_s^+ background events are modeled by using a Fermi function:

$$f(M_m^2) = \frac{1}{e^{[(M_m^2 - M_0^2)/E_C]} + 1}, \tag{2}$$

where M_0^2 represents the M_m^2 dropoff value and E_C the smearing of the Fermi edge. The values for M_0^2 and E_C, $M_0^2 = (0.303 \pm 0.034)\ \mathrm{GeV}^2/c^4$ and $E_C = (0.333 \pm 0.018)\ \mathrm{GeV}^2/c^4$ for the electron channel and $M_0^2 = (0.247 \pm 0.041)\ \mathrm{GeV}^2/c^4$ and $E_C = (0.346 \pm 0.022)\ \mathrm{GeV}^2/c^4$ for the muon channel, are fixed to the values derived from fits to MC distributions and are the same for all D_s^+ decay chains. Signal events are modeled by a Gaussian distribution, with the same mean and width for all reconstruction channels. The width is fixed to the value determined from the simulation. The mean of the distribution is determined in the fit, allowing for contributions from events with a D_s^{*+} in the final state.

The total number of events with a D_s^+ and the number of combinatorial background events in the signal region have been determined from fits to the $m(D_s^+)$ distributions. The number of signal $B^- \to D_s^{(*)+} K^- \ell^- \bar{\nu}_\ell$ and D_s^+ background events are extracted from the fits to the M_m^2 distributions, separately for the electron and muon samples. For these fits the three D_s^+ decay channels are combined, taking into account their detection branching fractions $\epsilon_\mathrm{BR} = \mathcal{B}(D_s^+ \to D1d2) \times \mathcal{B}(D1 \to d3d4)$ and individual reconstruction efficiencies ϵ_reco. For illustration, these efficiencies and the branching ratios are listed in Table I, together with the total fitted number of signal events and the estimated contributions from each of the three channels.

The fit is performed in the range $|M_m^2| < 1.5\ \mathrm{GeV}^2/c^4$ and has 10 free parameters: the mean value of M_m^2, the total number of fitted signal events N^signal, five parameters that describe the shape of the combinatorial background, and three sideband normalization parameters. The number of signal and D_s^+ background events are free in the fit; only the sum of both values is constrained to the result of the fits to the $m(D_s^+)$ distributions.

The likelihood function is

$$\mathcal{L} = \frac{e^{-N^\mathrm{signal}}}{n!}(N^\mathrm{signal})^n \prod_j \prod_i^{N_j} \mathcal{P}(M_{m,i}^2, \alpha_j), \tag{3}$$

TABLE I. Signal yields, selection efficiencies ϵ_{reco}, and branching fractions $\epsilon_{\text{BR}} = \mathcal{B}(D_s^+ \to D1d2) \times \mathcal{B}(D1 \to d3d4)$ for the individual and combined decay chains. The signal yields of each decay chain are computed by using N^{signal} and the efficiencies and are given for illustration only. The errors on the signal yields are the fit errors, the uncertainties of ϵ_{reco} are the systematic uncertainties, and the uncertainties of ϵ_{BR} represent the limited knowledge of the branching fractions of the D_s^+.

D_s^+ decay chain	$N^{\text{signal}}_{\text{electron}}$	$\epsilon_{\text{reco,electron}}$ [%]	$N^{\text{signal}}_{\text{muon}}$	$\epsilon_{\text{reco,muon}}$	ϵ_{BR} [%]
All	$259.4^{+67.6}_{-67.2}$		$209.7^{+53.0}_{-52.2}$		
$D_s^+ \to \phi\pi^+$, $\phi \to K^+K^-$	$115.7^{+30.2}_{-30.0}$	(2.76 ± 0.08)	$92.1^{+23.3}_{-22.9}$	(1.62 ± 0.06)	(2.18 ± 0.33)
$D_s^+ \to \bar{K}^{*0}K^+$, $\bar{K}^{*0} \to K^-\pi^+$	$85.2^{+22.2}_{-22.1}$	(1.79 ± 0.06)	$70.2^{+17.8}_{-17.5}$	(1.09 ± 0.05)	(2.60 ± 0.40)
$D_s^+ \to K_s^0K^+$, $K_s^0 \to \pi^+\pi^-$	$58.5^{+15.3}_{-15.2}$	(2.98 ± 0.08)	$(47.4^{+12.0}_{-11.8})$	(1.78 ± 0.06)	(1.02 ± 0.09)

with N_j the number of events and $\mathcal{P}(M^2_{m,i}\alpha_j)$ the probability density function (PDF) for a given fit slice j (signal region or sideband of each D_s^+ decay chain), with the fit parameters α, and $n = \sum_j N_j$ the total number of events.

By using MC experiments from a generator, which includes parameterizations of detector performance for signal reconstruction and background expectations, it has been verified that the fit is able to extract signal branching fractions for $\mathcal{B}(B^- \to D_s^{(*)+}K^-\ell^-\bar{\nu}_\ell) > 3 \times 10^{-4}$. Values of fit biases are also determined with this procedure and are taken into account in the analysis.

Fit results are given in Table I. Reconstruction efficiencies for the three decay chains are obtained by counting simulated signal events in the range $|M_m^2| < 1.2\ \text{GeV}^2/c^4$. As reported in Ref. [19], the reconstruction efficiency of the $D_s^+ \to \phi\pi^+$ decay chain depends on the requirement on the ϕ mass. The impact of this effect is covered by the systematic uncertainties on ϵ_{BR}. Figure 2 shows the sideband subtracted M_m^2 distributions summed over the decay channels.

The bias-corrected signal yields are $N^{\text{signal}}_{\text{electron}} = 301^{+68}_{-67}$ and $N^{\text{signal}}_{\text{muon}} = 206^{+53}_{-52}$. The bias correction is $+42$ (-4) events for the electron (muon) channel. Extended simulations showed that the source of the bias is a fluctuation of the underlying combinatorial background distribution.

The systematic uncertainties are divided into two categories: Additive uncertainties (Table II) are related to the number of extracted signal events, while multiplicative uncertainties (Table III) are related to the calculated branching fraction. The uncertainty due to the D_s^+ daughter branching fractions is quoted separately.

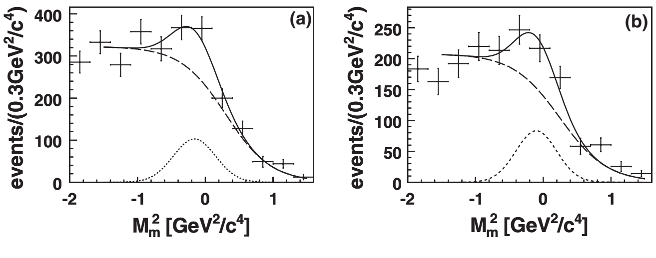

FIG. 2. Sideband subtracted M_m^2 distributions with fitted functions superimposed: (a) for the electron channel and (b) for the muon channel. All D_s^+ reconstruction chains have been summed. Solid lines represent the full distribution, dashed lines are the D_s^+ background component, and dotted lines represent the fitted signal component.

The systematic uncertainty arising from the choice of the D_s^+ background PDF is evaluated by using 1000 statistically independent MC experiments. Each experiment corresponds to different values for the two parameters that describe the PDF, M_0^2 and E_C, which are distributed according to the error matrix for these parameters. We take the width of a Gaussian fitted to the resulting N^{signal} distribution as a systematic uncertainty. The impact of shape differences between the data and MC simulations has been studied, as well as shape differences due to varying compositions of the D_s^+ background, and both were found to be negligible. A similar procedure is used to estimate the uncertainty due to using the D_s^+ branching fractions ϵ_{BR} for the combination of the individual channel signal yields. MC samples of ϵ_{BR} are produced for each decay channel by using the information of Ref. [1]. This leads to differences in the total number of extracted signal events. The width of a Gaussian fitted to the resulting distribution of signal yields is taken as the systematic uncertainty.

The width of the Gaussian PDF of M_m^2 for the signal and the number of fitted D_s^+ are varied by $\pm 1\sigma$ to evaluate these systematic uncertainties. This approach also takes into account the variation of the width due to a contribution of D_s^{*+} to the signal yield. The systematic uncertainty related to the bias correction is given by the statistical uncertainty of the correction.

We evaluate the uncertainty of the signal MC model by calculating the difference of the efficiencies between the

TABLE II. Additive systematic uncertainties in events.

Source	$\Delta N_{\text{elec.}}$ [evts]	ΔN_{muon} [evts]
D_s^+ bkg parameterization	19.9	15.9
Single channel signal yields	14.5	9.0
Width of the signal PDF	3.9	4.3
Error of the $m(D_s^+)$ fits	3.6	3.4
Total, affecting significance	25.2	19.1
Bias correction	2.2	1.8
Total uncertainty	25.3	19.2

TABLE III. Multiplicative systematic uncertainties in percent.

Source	Syst. uncer. electron (muon) ch. [%]		
	$\phi\pi^+$	$\bar{K}^{*0}K^+$	$K_S^0K^+$
Signal MC model	7.6 (0.2)	3.1 (6.4)	5.9 (2.1)
N (signal MC)	2.7 (3.5)	3.3 (4.2)	2.5 (3.3)
Particle ID	0.6 (1.6)	1.2 (4.9)	3.6 (7.9)
K_S^0 eff.	$\cdots$ ($\cdots$)	$\cdots$ ($\cdots$)	2.0 (3.1)
Tracking eff.	0.4 (0.1)	0.5 (0.2)	1.8 (2.4)
Photon eff.	0.6 (0.9)	0.4 (0.9)	0.5 (0.7)
Radiative corr.	2.0 (2.1)	2.2 (2.5)	1.9 (1.9)
Total $\Delta\epsilon_{\text{reco}}$	8.4 (4.5)	5.2 (9.5)	8.1 (9.9)
B counting	1.1 (1.1)	1.1 (1.1)	1.1 (1.1)
$\mathcal{B}$ (D_s^+)	15.1 (15.1)	15.4 (15.4)	6.0 (6.0)

alternative signal models and the Goity-Roberts signal MC model. The impact of the finite statistics of the simulated signal sample is deduced from the uncertainty on the efficiency determination. The uncertainty arising from particle identification, as well as from the K_S^0 reconstruction, is determined by using dedicated high purity control samples for the corresponding particles. Uncertainties arising from track and photon reconstruction, as well as from radiative corrections, are evaluated by varying their reconstruction efficiencies and the energy radiated by photons in the simulation. The uncertainty on the number of B mesons in the data set is determined as described in Ref. [20], and the D_s^+ daughter branching fraction uncertainties are taken from Ref. [1].

A second fit, imposing an $N^{\text{signal}} = 0$ hypothesis, is used to estimate the significance of the measurement. Since the mean of the Gaussian is a free parameter in the signal PDF, the difference in the number of free parameters (ΔNDF) of the fits is larger than 1. As shown in Ref. [21], the resulting probability distribution cannot be approximated by a chi-square distribution with an integer number of degrees of freedom. Thus, only a significance range, representing the significances for $\Delta NDF = 2$ and $\Delta NDF = 1$, is calculated. Including statistical and systematic uncertainties, the ranges are $[3.3\text{–}3.7]\sigma$ and $[3.5\text{–}3.9]\sigma$ for the electron and muon channel, respectively. Combining both lepton channels results in a significance larger than 5.0σ.

The branching fractions for the individual lepton channels are $\mathcal{B}(B^- \to D_s^{(*)+} K^- e^- \bar{\nu}_e) = [5.81^{+1.30}_{-1.30}(\text{stat}) \pm 0.54 (\text{syst}) \pm 0.49(\mathcal{B}(D_s))] \times 10^{-4}$ and $\mathcal{B}(B^- \to D_s^{(*)+} K^- \mu^- \bar{\nu}_\mu) = [6.68^{+1.72}_{-1.69}(\text{stat}) \pm 0.69(\text{syst}) \pm 0.56(\mathcal{B}(D_s))] \times 10^{-4}$, where the last uncertainty reflects the limited knowledge of the D_s branching fractions. The measurements are combined, taking into account the correlations between their systematic uncertainties, yielding $\mathcal{B}(B^- \to D_s^{(*)+} K^- \ell^- \bar{\nu}_\ell) = [6.13^{+1.04}_{-1.03}(\text{stat}) \pm 0.43(\text{syst}) \pm 0.51(\mathcal{B}(D_s))] \times 10^{-4}$.

In summary, using a data sample of about 376.9×10^6 $B\bar{B}$ pairs, we find evidence for the decay $B^- \to D_s^{(*)+} K^- \ell^- \bar{\nu}_\ell$. The signal has a significance larger than 5.0σ, after taking systematic effects into account. The measured branching fraction $\mathcal{B}(B^- \to D_s^{(*)+} K^- \ell^- \bar{\nu}_\ell) = [6.13^{+1.04}_{-1.03}(\text{stat}) \pm 0.43(\text{syst}) \pm 0.51(\mathcal{B}(D_s))] \times 10^{-4}$, where the last uncertainty reflects the limited knowledge of the D_s branching fractions, is consistent with the previous upper limit reported by the ARGUS Collaboration and with theoretical expectations.

We are grateful for the excellent luminosity and machine conditions provided by our PEP-II colleagues and for the substantial dedicated effort from the computing organizations that support *BABAR*. The collaborating institutions thank SLAC for its support and kind hospitality. This work is supported by DOE and NSF (USA), NSERC (Canada), CEA and CNRS-IN2P3 (France), BMBF and DFG (Germany), INFN (Italy), FOM (The Netherlands), NFR (Norway), MES (Russia), MICIIN (Spain), and STFC (United Kingdom). Individuals have received support from the Marie Curie EIF (European Union), the A. P. Sloan Foundation (USA), and the Binational Science Foundation (U.S.–Israel).

---

[*] Present address: Temple University, Philadelphia, PA 19122, USA.

[†] Also with Università di Perugia, Dipartimento di Fisica, Perugia, Italy.

[‡] Also with Università di Roma La Sapienza, I-00185 Roma, Italy.

[§] Present address: University of South Alabama, Mobile, AL 36688, USA.

[‖] Also with Università di Sassari, Sassari, Italy.

[1] C. Amsler *et al.* (Particle Data Group), Phys. Lett. B **667**, 1 (2008).

[2] B. Aubert *et al.* (*BABAR* Collaboration), Phys. Rev. Lett. **100**, 151802 (2008).

[3] B. Aubert *et al.* (*BABAR* Collaboration), Phys. Rev. Lett. **101**, 261802 (2008).

[4] D. Liventsev *et al.* (Belle Collaboration), Phys. Rev. D **77**, 091503 (2008).

[5] J. Abdallah *et al.* (DELPHI Collaboration), Eur. Phys. J. C **45**, 35 (2006).

[6] N. Uraltsev, Phys. Lett. B **501**, 86 (2001).

[7] Throughout this Letter, whenever a mode is given, the charge conjugate is implied.

[8] E. Golowich *et al.*, Z. Phys. C **48**, 89 (1990).

[9] P. Abreu *et al.* (DELPHI Collaboration), Phys. Lett. B **289**, 199 (1992).

[10] H. Albrecht *et al.* (ARGUS Collaboration), Z. Phys. C **60**, 11 (1993).

[11] B. Aubert *et al.* (*BABAR* Collaboration), Nucl. Instrum. Methods Phys. Res., Sect. A **479**, 1 (2002).

[12] S. Agostinelli *et al.* (GEANT4 Collaboration), Nucl. Instrum. Methods Phys. Res., Sect. A **506**, 250 (2003).

[13] J. L. Goity and W. Roberts, Phys. Rev. D **51**, 3459 (1995).

[14] N. Isgur, D. Scora, B. Grinstein, and M. Wise, Phys. Rev. D **39**, 799 (1989).

[15] A. Höcker *et al.*, Proc. Sci., ACAT (2007) 040.

[16] Throughout this Letter, all kinematic variables are defined in the center of mass frame.

[17] G. C. Fox and S. Wolfram, Phys. Rev. Lett. **41**, 1581 (1978).

[18] $L_2 = \sum_i |\vec{p}_i| \cos^2(\theta_i)$, where the sum is over all tracks in the event not used to form the signal B candidate and $\vec{p}_i$ and θ_i are the momenta and angles with respect to the thrust axis of the signal B candidate, respectively.

[19] J. P. Alexander *et al.* (CLEO Collaboration), Phys. Rev. Lett. **100**, 161804 (2008).

[20] B. Aubert *et al.* (*BABAR* Collaboration), Phys. Rev. D **67**, 032002 (2003).

[21] R. B. Davies, Biometrika **74**, 33 (1987).